Palaeoclimate ocean conditions shaped the evolution of corals and their skeletons through deep time

Andrea M. Quattrini [1,2 ✉], Estefanía Rodríguez [3], Brant C. Faircloth[4,5], Peter F. Cowman [6], Mercer R. Brugler [3,7], Gabriela A. Farfan[8], Michael E. Hellberg[4], Marcelo V. Kitahara [9,10], Cheryl L. Morrison [11], David A. Paz-García [12], James D. Reimer [13,14] and Catherine S. McFadden [1]

Identifying how past environmental conditions shaped the evolution of corals and their skeletal traits provides a framework for predicting their persistence and that of their non-calcifying relatives under impending global warming and ocean acidification. Here we show that ocean geochemistry, particularly aragonite–calcite seas, drives patterns of morphological evolution in anthozoans (corals, sea anemones) by examining skeletal traits in the context of a robust, time-calibrated phylogeny. The lability of skeletal composition among octocorals suggests a greater ability to adapt to changes in ocean chemistry compared with the homogeneity of the aragonitic skeleton of scleractinian corals. Pulses of diversification in anthozoans follow mass extinctions and reef crises, with sea anemones and proteinaceous corals filling empty niches as tropical reef builders went extinct. Changing environmental conditions will likely diminish aragonitic reef-building scleractinians, but the evolutionary history of the Anthozoa suggests other groups will persist and diversify in their wake.

Corals engineer entire reef-based ecosystems from shallow waters to the deep sea by their ability to form colonies and precipitate calcium carbonate ($CaCO_3$) skeletons. However, rapidly increasing levels of atmospheric CO_2 are acidifying and warming the world's oceans[1], suppressing calcification and growth rates of corals[2–4] while leading to net dissolution of calcified skeletons[5,6], thereby causing mass mortality and threatening the structure and diversity of reef ecosystems worldwide[7,8]. Investigating the evolutionary history of corals and their relatives can illuminate how past climatic and geochemical changes shaped the persistence and evolution of this group, and thus inform predictions of the fate of coral reef ecosystems.

Corals and sea anemones comprise the class Anthozoa, a metazoan lineage that diversified throughout the Phanerozoic (541 million years ago (Ma) to present), an eon marked by strong fluctuations in ocean geochemistry, sea surface temperatures and atmospheric CO_2 (ref. [8]). Throughout geologic time, ocean chemical conditions have cycled between aragonite and calcite seas, driven primarily by fluctuating Mg/Ca ratios. High Mg/Ca ratios (above ~2 molar Mg/Ca) favour the precipitation of aragonite and high-Mg calcite (HMC) while low Mg/Ca ratios (below ~2 molar Mg/Ca) favour the precipitation of low-Mg calcite (LMC)[9–11]. If ocean geochemistry was important in the evolution of different anthozoan skeletal types (Supplementary Table 1 and Extended Data Fig. 1), we expect aragonitic reef-building corals (scleractinians) to have

evolved when Mg/Ca ratios were high (aragonite seas) while we expect other anthozoans (for example, sea anemones, black corals, octocorals) with different skeletal types (for example, none, proteinaceous, calcitic) to have evolved during periods not conducive to aragonite precipitation (calcite seas).

In addition to oscillations in ocean geochemistry, sea surface temperature and atmospheric CO_2 fluctuated throughout geologic time[8]. Global warming and ocean acidification (OA) events have been indicated as drivers in at least two of the five mass extinctions and two additional reef crises (that is, global declines in coral and other (for example, algal, sponge) reef builders) since the Ordovician (488–444 Ma)[12]. OA disproportionately impacts aragonitic and HMC-precipitating organisms, as these $CaCO_3$ forms have a higher measured apparent solubility constant in seawater than LMC[13,14]. In fact, coral reefs were most vulnerable to extinction under rapid increases in temperature and CO_2 combined with declines in aragonite saturation[8]. The loss of corals and other reef builders during these reef crises could have driven increases in the diversification rates of non-aragonitic or even non-calcifying anthozoans (for example, proteinaceous corals or sea anemones) as these more resilient[15] species invaded empty, shallow-water niches caused by the extinction of reef builders. For example, anemones and octocorals can overgrow coral reefs following a reduction in live coral cover[16,17] and can dominate areas with naturally high partial pressure of CO_2 (p_{CO_2}) conditions[18]. Identifying the changes

[1]Biology Department, Harvey Mudd College, Claremont, CA, USA. [2]Department of Invertebrate Zoology, National Museum of Natural History, Smithsonian Institution, Washington DC, USA. [3]Division of Invertebrate Zoology, American Museum of Natural History, New York, NY, USA. [4]Department of Biological Sciences, Louisiana State University, Baton Rouge, LA, USA. [5]Museum of Natural Science, Louisiana State University, Baton Rouge, LA, USA. [6]ARC Centre of Excellence for Coral Reef Studies, James Cook University, Townsville, Queensland, Australia. [7]Department of Natural Sciences, University of South Carolina Beaufort, Beaufort, SC, USA. [8]Department of Mineral Sciences, National Museum of Natural History, Smithsonian Institution, Washington DC, USA. [9]Institute of Marine Science, Federal University of São Paulo, Santos, Brazil. [10]Centre for Marine Biology, University of São Paulo, São Sebastião, Brazil. [11]US Geological Survey, Leetown Science Center, Kearneysville, WV, USA. [12]CONACyT-Centro de Investigaciones Biológicas del Noroeste (CIBNOR), Laboratorio de Necton y Ecología de Arrecifes, La Paz, México. [13]Molecular Invertebrate Systematics and Ecology Laboratory, Department of Marine Science, Chemistry, and Biology, Faculty of Science, University of the Ryukyus, Nishihara, Japan. [14]Tropical Biosphere Research Center, University of the Ryukyus, Nishihara, Japan. ✉e-mail: quattrinia@si.edu

in environmental conditions that shaped diversification of calcified and non-calcified anthozoans throughout deep time provides a framework to understand evolutionary persistence of corals and their relatives following impending global ocean change.

Here we examined whether fluctuations in aragonite–calcite seas promoted the gain or loss of different skeletal features in anthozoans. To test this hypothesis, we constructed a time-calibrated phylogeny of 234 anthozoans, with representatives from all orders and most families (Supplementary Table 2), using 1,729 loci captured with a targeted-enrichment approach (Supplementary Table 3). With this phylogeny, we also tested whether diversification rates increased following shifts between aragonite and calcite seas or after ocean warming and OA events and whether rate increases were more apparent in non-calcifying anthozoans during times when calcification would have been difficult.

Time-calibrated phylogeny

Our phylogeny unequivocally supports the Precambrian origin of Anthozoa and the reciprocal monophyly of subclasses Hexacorallia and Octocorallia (Fig. 1, Supplementary Table 4 and Extended Data Fig. 2). Both the multi-species coalescent (ASTRAL) species tree (Extended Data Fig. 3) and concatenated maximum likelihood (ML) phylogenies were congruent at deep nodes in the phylogeny, generally with strong support (> 95% bootstrap support or posterior probability > 0.95; Fig. 1 and Supplementary Information). Within Hexacorallia, we recovered monophyly of each order (Ceriantharia (tube anemones), Zoantharia (colonial anemones), Actiniaria (true sea anemones), Antipatharia (black corals), Corallimorpharia (naked corals, mushroom anemones), Scleractinia (stony corals), plus the enigmatic anemone-like *Relicanthus*), with Ceriantharia sister to all other hexacorals, similar to other phylogenomic studies[19,20], but in contrast to work based on mitogenomes[21]. Relationships within Octocorallia (sea fans, soft corals, sea pens) are largely congruent with those obtained from analyses of mitochondrial DNA[22] or nuclear ribosomal DNA[23], but with strong support for the deeper nodes in both major clades, almost all of which have lacked significant support in previous studies. Robust age estimates and strong support for phylogenetic relationships within and among these morphologically diverse clades now enable a more thorough examination of skeletal character evolution across deep time.

Skeletal trait evolution

Multiple gains and/or losses of different skeletal traits were apparent across Anthozoa, a clade whose most recent common ancestor lacked a skeleton (Fig. 1). Within Hexacorallia, the ancestral character state was also no skeleton. Skeletons of aragonite (Scleractinia) and scleroprotein (Antipatharia) were each gained once, with no reconstructed losses. The naked coral hypothesis that suggests corallimorpharians are derived from scleractinians by skeletal loss[24] was not supported, similar to another phylogenomic study[20] (Fig. 1).

In contrast to Hexacorallia, Octocorallia exhibits many different skeletal forms that have been gained and lost multiple times (Fig. 1). Most octocorals have sclerites—free skeletal elements of HMC that are embedded within the tissue—regardless of whether or not they have calcified or proteinaceous axes. Sclerites are present in early-diverging lineages of both major clades of octocorals, although they have been lost several times (that is, those octocorals with 'none'; Fig. 1). Skeletal axes comprised primarily of solid HMC (for example, suborder Calcaxonia) or of protein (for example, suborder Holaxonia) have rarely been gained but have frequently been lost, while axes of unconsolidated or consolidated sclerites ('Scleraxonia') have been gained multiple times in both major lineages (Fig. 1). Aragonite has also been gained at least twice in octocorals: in the order Helioporacea, which has a massive aragonitic skeleton analogous to Scleractinia, and in the family Primnoidae, whose central axes are composed of aragonite (Fig. 1). Aragonite

can also occur in the holdfasts of octocorals or embedded within a proteinaceous axis[25]. The evolutionary lability of skeletal composition and form within the Octocorallia suggests a greater ability to adapt readily to changes in ocean chemistry over deep time compared with the homogeneous, aragonitic Scleractinia.

The origin and evolution of different skeletal features coincide predominantly with periods of aragonite or calcite seas. The crown groups of hexacorals that lack skeletons, including Actiniaria, Ceriantharia and Zoantharia, originated primarily during calcite seas of the early to mid-Palaeozoic, as evidenced by mean ages (Supplementary Table 4) and the majority of the age distributions (Fig. 2a). During this time, calcite seas also corresponded with high levels of atmospheric CO_2 that perhaps posed challenges for calcification (Fig. 2).

Octocorals with only free HMC sclerites and those with both sclerites and highly calcified axes of HMC also arose during calcite seas and high CO_2 conditions of the early to mid-Palaeozoic (Fig. 2b). The evolution of calcitic skeletons under these conditions suggests strong biological control over calcification. Indeed, experimental studies have shown that octocorals can calcify under high p_{CO_2} conditions[18] and that their tissue protects them from OA[26]. Although extant octocorals precipitate HMC, which is favoured during high Mg/Ca ratios, it is also possible that HMC formed during the low Mg/Ca ratios[27] of the past. Moreover, extant organisms that precipitate HMC have been shown experimentally to switch to LMC in calcite seas[28], suggesting groups that evolved to precipitate LMC during past calcite seas could have facultatively switched to precipitate the HMC polymorph under present-day aragonite seas. In addition, the aragonite-producing Helioporaceae evolved during the late Jurassic–early Cretaceous, a time period characterized by calcite seas. Their skeletomes (proteins associated with skeletonization) are more similar to those of other HMC-secreting octocorals than to the aragonitic scleractinians[29], perhaps reflecting a later transition from precipitation of HMC to aragonite as sea states changed. Extant helioporaceans still produce sclerites of HMC in addition to a massive framework of aragonite. This ability to calcify under high p_{CO_2} conditions, calcify a variety of skeletal types and/or to facultatively switch between various $CaCO_3$ polymorphs endows octocorals with the capacity to adapt to ocean chemical changes.

Rugosans and tabulates—two groups of extinct hexacorals with calcitic skeletons—first appeared in the fossil record during the Ordovician, a time of calcite seas[30]. Scleractinia, which includes all extant stony corals, originated at the transition between calcite to aragonite seas (383 Ma, 95% confidence interval 324–447 Ma; Supplementary Table 4), but both crown clades of scleractinians ('robust' and 'complex', Figs. 1 and Fig. 2a) originated during the aragonite seas of the Carboniferous, when temperature and CO_2 also decreased (332–357 Ma; Supplementary Table 4). Scleractinians have persisted throughout the Mesozoic and Cenozoic eras, which have included intervals of calcite sea conditions unfavourable for the precipitation of aragonite. Survival of these scleractinian lineages during calcite seas may have been mediated by strong physiological and/or physicochemical control over the process of calcification[30–32], slower growth rates[33] or the ability to precipitate calcite in low Mg/Ca seas[34], and/or the potential for aragonite biomineralization in warm-water environments (>20 °C)[9]. Nevertheless, the evolution of aragonite skeletons in hexacorals during a time of aragonite sea conditions was a key innovation that, combined with coloniality and photosynthetic symbionts, enabled reef building and the evolutionary success of Scleractinia.

Diversification rates across deep time

The diversification rates of anthozoans (see also Supplementary Information) responded to mass extinctions and reef crises (Extended Data Fig. 4a, Akaike information criterion (AIC) = 4,773.9). Diversification rates increased following four
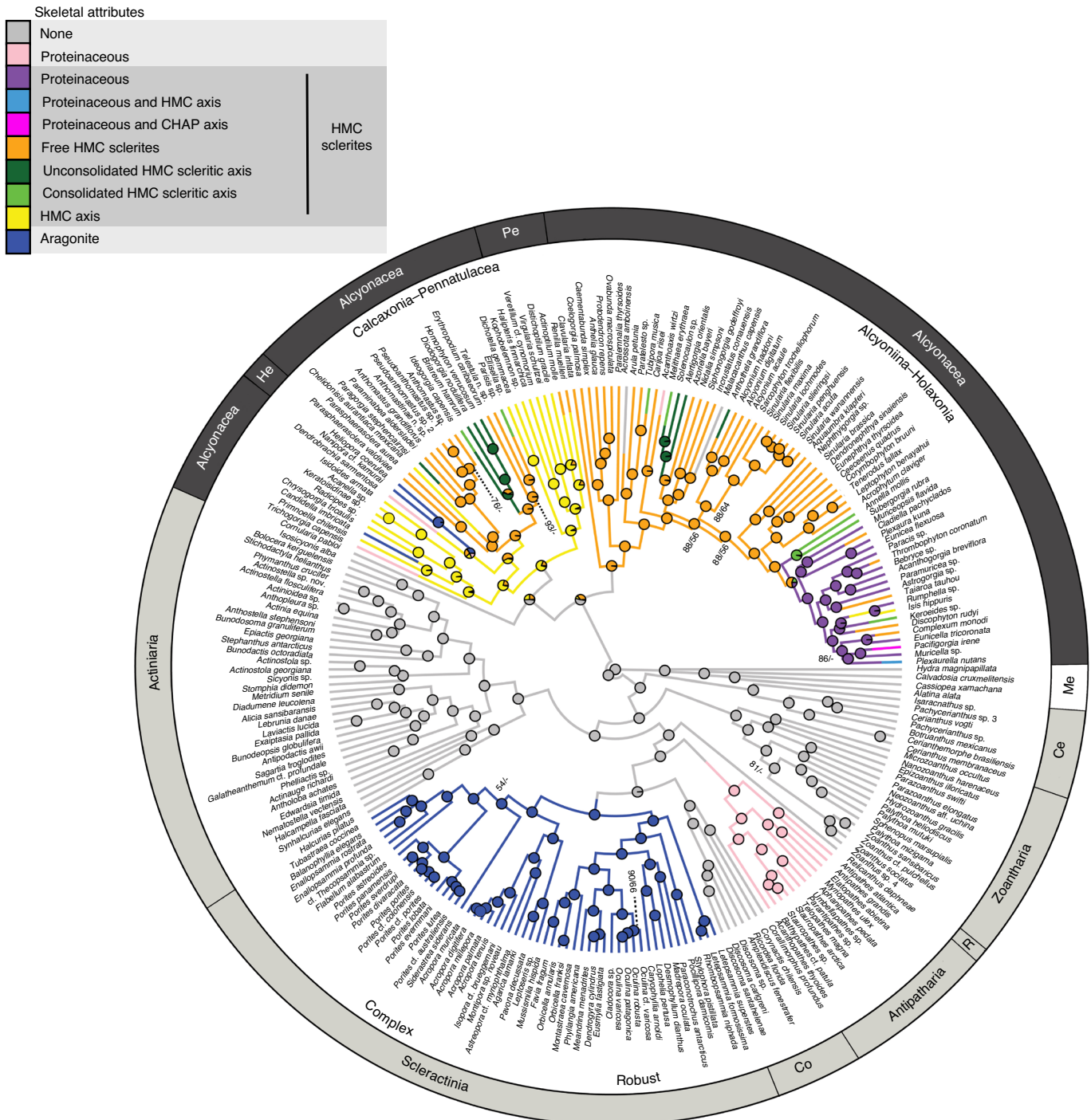
Fig. 1 | Phylogeny of Anthozoa with ancestral character states of skeletal types. Subclasses are colour coded (dark grey bars, Octocorallia; light grey bars, Hexacorallia) and orders are indicated (Ce, Ceriantharia; Co, Corallimorpharia; He, Helioporacea; Pe, Pennatulacea; R, *Relicanthus*). Medusozoan (Me) outgroup is indicated in white. Topology was produced from RAxML analysis of a 50% data matrix (933 loci, 278,819 bp). Bootstrap support was >95% at nodes in one or both of the phylogenies constructed with the 50% or 75% data matrices, unless indicated (bootstrap support from 50/75% data matrices). CHAP, amorphous carbonate hydroxylapatite.

of the five mass extinction events (late Devonian (374.5 Ma), Permian–Triassic (251 Ma), end-Triassic (199.6 Ma) and Cretaceous–Palaeogene (65.5 Ma)), the first three of which were also reef crises (Fig. 2 and Extended Data Fig. 4). Diversification rates also increased following two additional reef crises (early Jurassic (183 Ma) and Palaeocene–Eocene (55.8 Ma)) that disproportionally impacted reef builders[12]. OA and/or global warming caused all reef crises, except for the late Devonian extinction,

which was driven by widespread anoxia[12]. Increased diversification rates in anthozoans were perhaps due to expansion into new ecological niches[35] following extinction events and reef crises. The fossil record indicates that the majority of reef-building corals went extinct during the end-Triassic event[12,36,37]. Notably, it has been hypothesized that Helioporacea might fill empty niches following the demise of scleractinians[38], and indeed, this clade evolved following the end-Triassic and early-Jurassic reef crises.
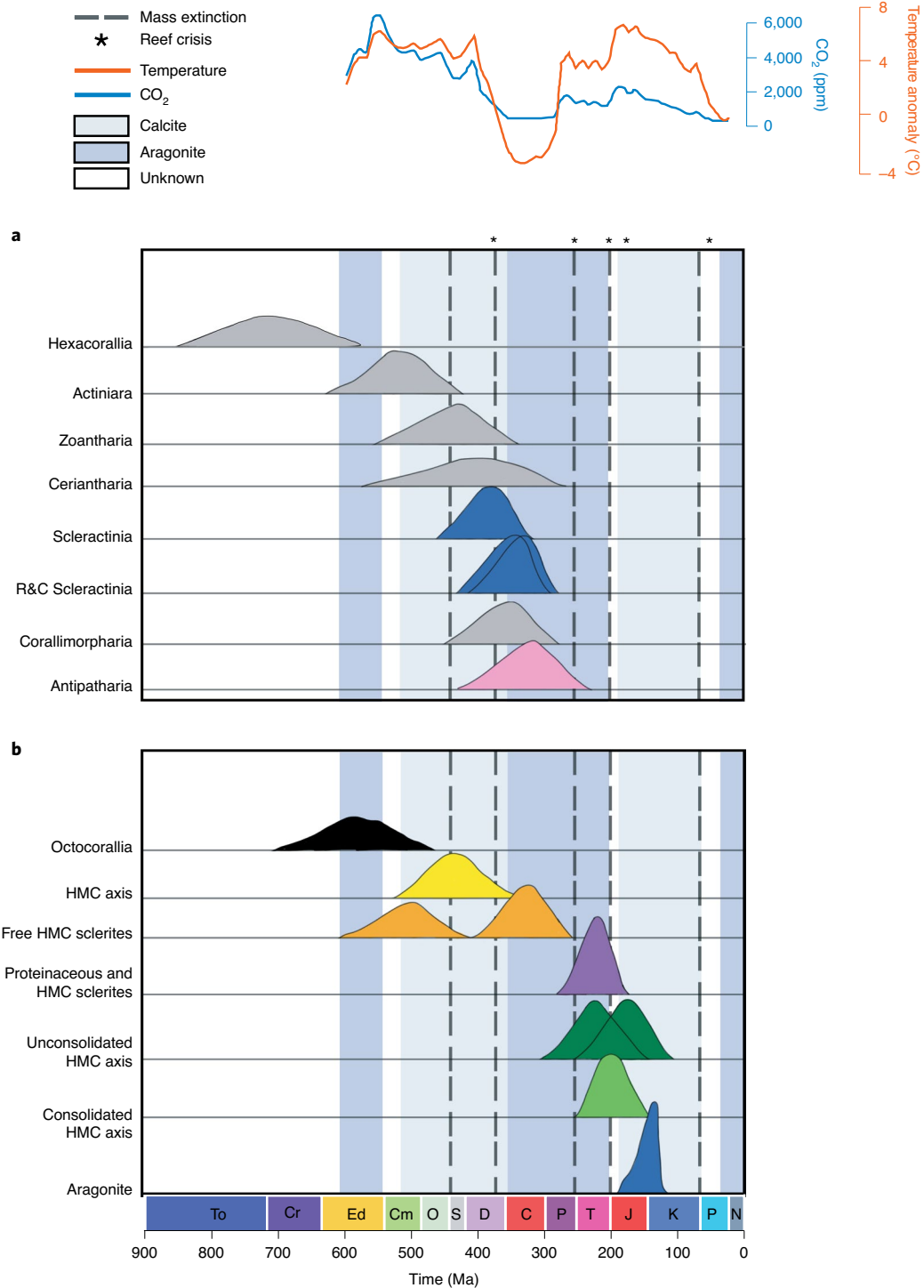
Fig. 2 | Timing and origin of anthozoans and their skeletal features across time and palaeoclimate ocean conditions. a,b, The 95% highest posterior densities for ages of crown groups within Hexacorallia (**a**) and crown groups within Octocorallia (**b**). Crown groups of Octocorallia correspond loosely to subordinal clades defined by skeletal composition, represented here by ancestral skeletal types with >75% posterior probability (Fig. 1). Colours of ancestral skeletal types: black, unknown; grey, none; blue, aragonite (Scleractinia, Helioporacea); pink, proteinaceous (Antipatharia); yellow, HMC calcite axes (Calcaxonia); orange, free HMC sclerites only (Alcyoniina, Stolonifera); purple, proteinaceous axis with HMC sclerites (Holaxonia); dark green, unconsolidated HMC axes (Scleraxonia); light green, consolidated HMC axes (Scleraxonia). R&C, robust and complex. Aragonite and calcite sea conditions follow refs. [8,9]. Geological era abbreviations: To, Tonian; Cr, Cryogenian; Ed, Ediacaran; Cm, Cambrian; O, Ordovician; S, Silurian; D, Devonian; C, Carboniferous; P, Permian; T, Triassic; J, Jurassic; K, Cretaceous; P, Palaeogene; N, Neogene. CO_2 and temperature curves adapted with permission from ref. [8], AAAS.

Aragonite–calcite sea changes were less important than mass extinctions and reef crises in driving diversification rates of Anthozoa (Extended Data Fig. 4b, AIC = 4,774.9). Although net diversification

rates increased at a few times when ocean chemical conditions changed (Devonian–Carboniferous (358 Ma), end-Triassic and Palaeogene–Neogene (40 Ma) boundaries), mass extinctions and
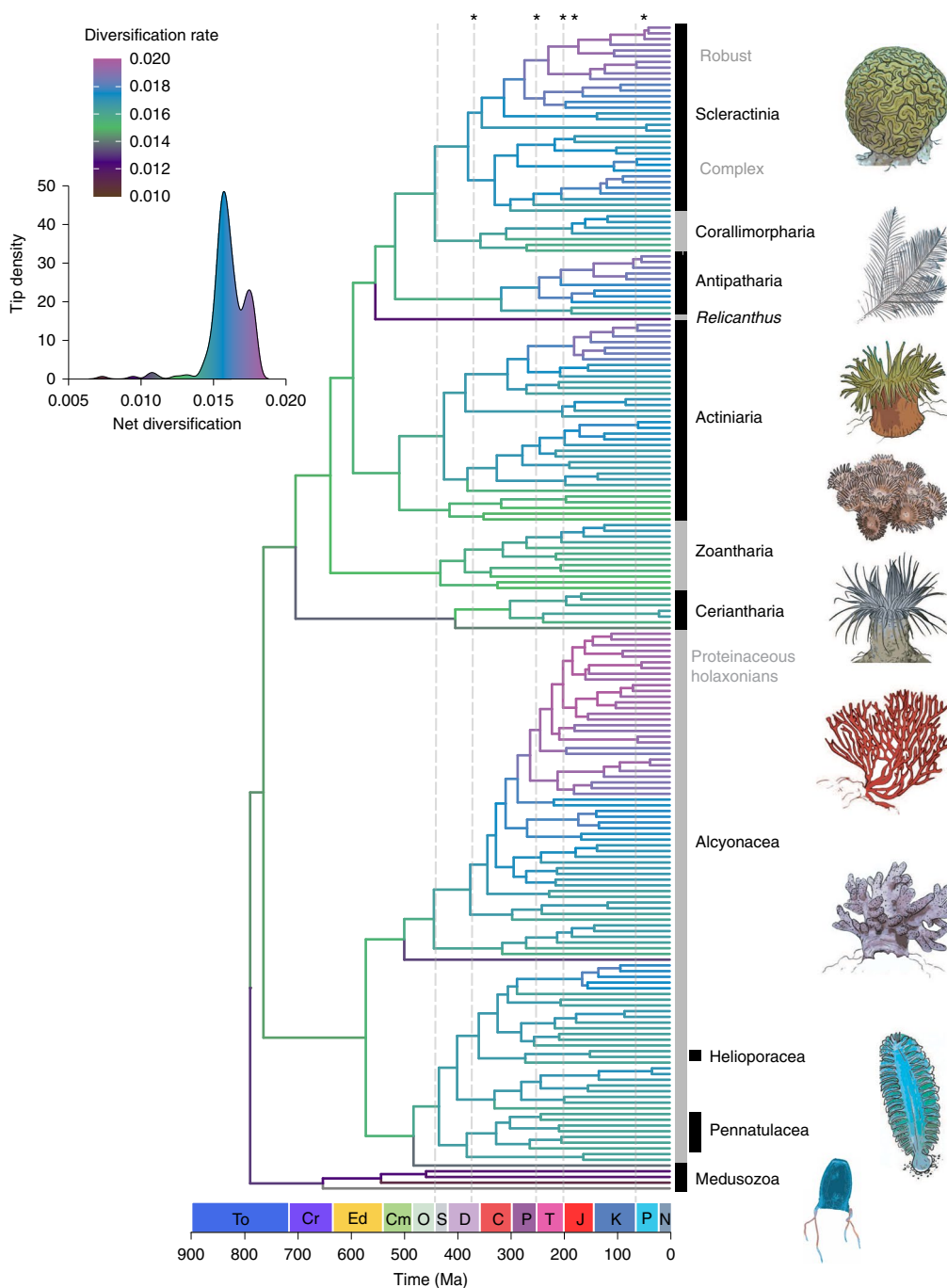
Fig. 3 | Branch-specific diversification rates across Anthozoa. Mass extinctions (dotted line) and reef crises (*) are shown. The density distribution of net diversification rates estimated at all the tips across the dated phylogeny is included in the upper left.

reef crises better explain the patterns observed (Extended Data Fig. 4). Devonian–Carboniferous and end-Triassic rate shifts coincide not only with aragonite–calcite sea transitions but also with mass extinction events that occurred concurrently. A pronounced increase in diversification rate at the Palaeogene–Neogene boundary, however, is associated with a change from calcite to aragonite seas and decreased ocean temperatures (Fig. 2 and Extended Data Fig. 4). This change may have enabled extant scleractinians to diversify during conditions that were suitable to calcification.

Increased diversification rates were more apparent in some clades of anthozoans than others (Fig. 3). In particular, rates of diversification were increased in 'robust' Scleractinia compared with 'complex' Scleractinia (Fig. 3). Notably, 'robust' corals have different biomineralization enzymes and transporters compared with 'complex' corals[39], promoting calcification in waters undersaturated with aragonite, such as the deep sea. The early-diverging lineage (Micrabaciidae) of robust corals (Fig. 1) occurs in deep waters (>200 m)[40] and many other robust corals build reefs in deep waters at or near the aragonite saturation horizon[41]. During reef crises (particularly at the end-Triassic extinction event), tropical taxa suffered more than temperate ones[12,36,37], but robust corals might have survived in deep water and/or high-latitude refugia[36] and rapidly diversified into shallower waters, including the Atlantic Ocean as it began to form.

Increased diversification rates were also evident in several groups of anthozoans that exhibit little to no calcification (Fig. 3). Rates of diversification increased in antipatharian black corals and holaxonian octocorals, which both have flexible proteinaceous skeletons with little to no calcitic material, in one clade of alcyoniin soft corals and in one group of actiniarian anemones that is primarily found in the shallow, tropical Atlantic. As evidenced by experimental studies[15,18] these groups of anthozoans likely had higher adaptive capacity for OA, warming temperatures and calcite seas, and perhaps rapidly diversified following the extinction of scleractinians and other reef builders during reef crises.

In summary, we show that evolutionary diversification of anthozoans and their skeletal attributes shifted across geologic time in response to palaeoclimate conditions. Aragonite skeletons biomineralized by scleractinians arose during aragonite seas whereas non-calcifying and primarily calcitic anthozoans evolved during calcite sea intervals with high levels of atmospheric CO_2. Increased diversification rates were largely coupled with mass extinction events and reef crises, known to cause major restructuring of the biosphere. Certain anthozoan groups, in particular robust corals, the non-skeletonized actiniarian anemones, and antipatharians and octocorals with largely proteinaceous skeletons, fared better during and immediately following these events compared with the reef-building, tropical scleractinians, perhaps due to higher adaptive capacity in response to environmental change coupled with new ecological opportunities. In fact, we are currently witnessing phase shifts to octocoral-dominated communities where scleractinians have declined[42], as octocorals appear to have greater resiliency to ongoing environmental change[16,18]. Projected global ocean change will undoubtedly impact coral ecosystem functioning and biodiversity, particularly reef-building scleractinians, but these lessons from the deep past suggest that other anthozoan-dominated communities will persist and prosper in their place.

Methods

Library preparation and target enrichment. DNA was extracted from specimens collected worldwide from 1991 to 2018 (Supplementary Table 2) using a Qiagen DNeasy Blood and Tissue kit, Qiagen Gentra Kit, or a CTAB extraction protocol (for older or degraded samples). For black corals and a few scleractinians, a Qiagen DNEasy Pro Power Clean kit was used to remove PCR inhibitors. Samples with high-molecular-weight DNA were sheared to a target size range of 400–800 bp using sonication (Q800R QSonica sonicator). A total of 250 ng at a concentration of 10 ng μl⁻¹ per sample was used in library preparation. Small DNA fragments were removed from each sample using a 3:1 generic SPRI substitute bead cleanup. DNA was re-suspended in 25 μl of nuclease-free water. Library preparation (Kapa Biosystems) was conducted with a Kapa Hyper Prep protocol using universal Y-yoke oligonucleotide adapters and custom iTru dual-indexed primers. Five to eight libraries were pooled at equimolar ratios to a total of 500 ng per pool for target enrichment. The anthozoan-v1 bait set[43] or hexacoral-v2-scleractinian bait set[44] was used to enrich ultraconserved elements and exons. Baits were diluted to 1/2 (250 ng) of the standard (500 ng) MyBaits concentration. Enriched libraries were sequenced on an Illumina HiSeq 3000 (150 bp PE reads, two lanes). Additional library preparation and target enrichment details can be found in Quattrini et al.[43] and Cowman et al.[44].

Bioinformatic analyses. De-multiplexed Illumina reads were processed using PHYLUCE[45] following the workflow in the online tutorial (http://phyluce. readthedocs.io/en/latest/tutorial-one.html/), with a few modifications (see Quattrini et al.[43]). Briefly, the reads were trimmed using the Illumiprocessor wrapper program[45] with default values and then assembled using SPAdes v 3.1[46] (with the —careful and —cov-cutoff 2 parameters). At this stage, we included 21 whole and partial genomes in the analysis, including four medusozoan outgroup taxa (Supplementary Table 2). 'Phyluce_assembly_match_contigs_to_probes' was used to match baits to contigs at a minimum coverage and minimum identity of 70%. Loci (Extended Data Fig. 5) were then extracted using 'phyluce_assembly_ get_fastas_from_match_counts' and aligned with default parameters using 'phyluce_align_seqcap_align'. Loci were internally trimmed with GBlocks using 'phyluce_align_get_gblocks_trimmed_alignments_from_untrimmed' (—b1 0.5, —b2-0.5, —b3 10, —b4 5). Data matrices of locus alignments were created using 'phyluce_align_get_only_loci_with_min_taxa', in which each locus had either 50% or 75% species occupancy. Data matrices were also constructed for hexacorals and octocorals only, with six outgroup taxa in each data matrix. Locus alignments were concatenated using 'phyluce_align_format_nexus_files_for_raxml'.

Phylogenetic analyses. Phylogenetic analyses were conducted using ML, Bayesian and species tree methods. ML inference was conducted on both 50% and 75% concatenated data matrices in RAxML v8[47], using rapid bootstrapping, which allows for a complete analysis (20 ML searches and 200 bootstraps, GTRGAMMA model) in one step. ML analyses were also conducted on 50% and 75% data matrices of hexacorals and octocorals only, with six outgroups in each analysis (outgroup species were chosen to maximize loci retained in analysis). Locus data were partitioned using PartitionFinder[48], using a GTRGAMMA model and linked branch lengths, with a corrected AIC model selection criterion. A partitioned analysis on concatenated data was conducted using rapid bootstrapping (GTRGAMMA model) in RAxML v8 on the CIPRES portal. Bayesian analysis was conducted on both 50% and 75% data matrices using ExaBayes[49] (100 M and 10 M generations, respectively, four chains, 25% burnin). The species tree analysis was conducted using ASTRAL III[50]. First, 220 gene trees (75% species occupancy alignments) were constructed using rapid bootstrapping in RAxML v8 (GTRGAMMA model). Trees were then concatenated into one file and TreeShrink[51] was used to remove long branches from gene trees. Finally, branches with low bootstrap support (<30%) were removed using a newick utility (nw_ed[52]) before input in ASTRAL III.

Divergence time estimation. Divergence dating was conducted in BEAST2 v2.5[53] on CIPRES. Six fossil calibration points (Supplementary Table 5) were selected for dating the anthozoan phylogeny after careful consideration to confirm that morphological characters of fossils unequivocally matched extant lineages. The fossil record for octocorals is particularly sparse, and most fossil taxa have been identified from sclerites alone, which are known to exhibit homoplasy. We used only fossils whose identity had been validated from diagnostic morphological characters other than sclerites. We also included a calibration at the root of the phylogeny for the earliest confirmed Cambrian fossil of a cnidarian (Supplementary Table 5). Exponential priors were used for calibration points following ref. [54] with minimum age constraints set as the offset values and mean values set as 10% of the offsets (except that the Keratoisidinae node was given a mean value of 20% of the offset and the root was given a mean value of 11% of the offset to capture potentially older ages found in previous studies). A relaxed clock model, with a lognormal distribution on the ucld.mean (initial 0.0002, 0-infinity bounds, following ref. [55]) and uniform distribution on the ucld.stdev (initial 0.1, 0–1 bounds), was used. A birth–death tree prior was also used, with uniform priors on the birth rate (initial 1.0, 0–1,000 bounds) and death rate (initial 0.5, 0–1 bounds); results were compared with a Yule model (Supplementary Information). Following Oliveros et al.[56], we used a fixed topology (Fig. 1) in BEAST2. Although the topologies were congruent at all deeper nodes in the tree, we used the RAxML topology from the 50% data matrix rather than the ASTRAL species tree or the 75% RAxML tree because of higher support for the majority of internal nodes. This topology was first time-calibrated with the above fossils (no root calibration) using a penalized likelihood method[57] in the R package ape. We also included only 25 loci in the BEAST2 analysis (as per Oliveros et al.[56]) that were determined to be clock-like, with properties of moderate tree lengths and topological similarity to the species tree, as determined using SortaDate[58]. Locus data were partitioned so that a GTRGAMMA model (initial 1.0, 0 to infinity bounds) was applied to each locus. Three separate runs of 250 M generations were conducted. Log and tree files from each run were combined in LogCombiner[53], with a 10% burnin. The combined log file was assessed for convergence of parameter values and age estimates by inspecting traces and effective sample sizes in Tracer v.1.7[59]. TreeAnnotator[53] was then used to produce a maximum clade credibility tree. An analysis (250 M generations) was also conducted without data by sampling from the prior, to ensure that the results were driven by the data and not solely by the prior information[60]. All BEAST2 analyses were conducted on CIPRES.

The combined tree file was resampled to randomly select 13,508 trees to obtain the 95% highest posterior distribution (HPD) of node ages for particular clades. Clades for which 95% HPDs were calculated included all hexacoral orders, as they were monophyletic and each represented by one skeletal type. Because of widespread polyphyly and paraphyly of currently recognized orders and suborders of octocorals, HPDs of node ages were calculated for monophyletic clades represented by ancestral skeletal types of >75% posterior probability (Fig. 2). These analyses, along with plotting of the posterior distributions, were conducted in R using an R script (J. Schenk, https://github.com/johnjschenk/Rcode/blob/master/ NodeAgeDensity.R).

Ancestral state reconstruction. Ancestral states of skeletal type were calculated using stochastic character mapping, which samples ancestral states from their posterior probability distribution[61]. Posterior probabilities were generated from 100 stochastic character maps for each trait using the make.simap function in the R package phytools[62]. Using phytools, one stochastic character map for skeletal traits (Fig. 1) was plotted on the time-calibrated phylogeny along with the posterior probabilities (pie charts) at each node.

Diversification rate analyses. Episodic diversification rates were calculated in RevBayes version 1.03[63] to determine whether diversification rates shifted across environmental conditions. Diversification rates were calculated between mass

extinction events and reef crises and between shifts in aragonite and calcite sea intervals. A uniform taxon sampling strategy was used, with incomplete taxon sampling accounted for by dividing the number of tips by the total number of anthozoan species (rho). Two MCMC runs were conducted for 500,000 generations (tuning interval 200); trace files were examined for convergence in Tracer v1.7[59]. To determine whether one model of episodic rate diversification was preferred over another, we calculated AIC for Markov chain Monte Carlo (MCMC) samples using the R package geiger[64]. Net diversification rates (speciation rates minus extinction rates) were plotted using the RevGadgets function (https://github.com/revbayes/RevGadgets) in R with the weighted average rate computed in each of 100 time intervals. Branch-specific diversification rates[65] were also calculated to determine whether branch rates ($k = 8$ discrete branch-rate categories) varied across the phylogeny. The phylogeny was pruned to one species per genus (except for the *Alcyonium* spp., which should be considered separate genera). Extinction rate was kept constant and a uniform incomplete taxon strategy was adopted as described above. Two MCMC runs were conducted for 2,500 generations; trace files were examined for convergence in Tracer v1.7[59]. More details can be found in Supplementary Information.

Reporting Summary. Further information on research design is available in the Nature Research Reporting Summary linked to this article.

Data availability
Raw data: NCBI Genbank BioProject# PRJNA413622 and PRJNA588468, BioSample #SAMN07774920-4952, 13244867-5050. Anthozoan bait set: Data Dryad Entry https://doi.org/10.5061/dryad.36n40. Alignment and tree files, BEAST2 xml and result files: figshare https://doi.org/10.6084/m9.figshare.12363953.

Code availability
Code is included on figshare https://doi.org/10.6084/m9.figshare.12363953.

References
1. IPCC *Climate Change 2007: The Physical Science Basis* (eds Solomon S. et al.) (Cambridge Univ. Press, 2007).
2. Kleypas, J. A. et al. Geochemical consequences of increased atmospheric carbon dioxide on coral reefs. *Science* **284**, 118–120 (1999).
3. De'ath, G., Lough, J. M. & Fabricius, K. E. Declining coral calcification on the Great Barrier Reef. *Science* **323**, 116–119 (2009).
4. Cantin, N. E., Cohen, A. L., Karnauskas, K. B., Tarrant, A. M. & McCorkle, D. C. Ocean warming slows coral growth in the central Red Sea. *Science* **329**, 322–325 (2010).
5. Kleypas, J. A. & Yates, K. K. Coral reefs and ocean acidification. *Oceanography* **22**, 108–117 (2009).
6. Eyre, B. D. et al. Coral reefs will transition to net dissolving before end of century. *Science* **359**, 908–911 (2018).
7. Carpenter, K. E. et al. One-third of reef-building corals face elevated extinction risk from climate change and local impacts. *Science* **321**, 560–563 (2008).
8. Pandolfi, J. M., Connolly, S. R., Marshall, D. J. & Cohen, A. L. Projecting coral reef futures under global warming and ocean acidification. *Science* **333**, 418–422 (2011).
9. Balthasar, U. & Cusack, M. Aragonite-calcite seas—quantifying the gray area. *Geology* **43**, 99–102 (2015).
10. De Choudens-Sanchez, V. & Gonzalez, L. A. Calcite and aragonite precipitation under controlled instantaneous supersaturation: elucidating the role of CaCO₃ saturation state and Mg/Ca ratio on calcium carbonate polymorphism. *J. Sediment. Res.* **79**, 363–376 (2009).
11. Ries, J. B. Geological and experimental evidence for secular variation in seawater Mg/Ca (calcite–aragonite seas) and its effects on marine biological calcification. *Biogeosciences* **7**, 2795–2849 (2010).
12. Kiessling, W. & Simpson, C. On the potential for ocean acidification to be a general cause of ancient reef crises. *Glob. Change Biol.* **17**, 56–67 (2011).
13. Morse, J. W., Mucci, A. & Millero, F. J. The solubility of calcite and aragonite in seawater of 35% salinity at 25°C and atmospheric pressure. *Geochim. Cosmochim. Acta* **44**, 85–94 (1980).
14. Morse, J. W., Andersson, A. J. & Mackenzie, F. T. Initial responses of carbonate-rich shelf sediments to rising atmospheric $p\text{CO}_2$ and "ocean acidification": role of high Mg-calcites. *Geochim. Cosmochim. Acta* **23**, 5814–5830 (2006).
15. Suggett, D. J. et al. Sea anemones may thrive in a high CO₂ world. *Glob. Change Biol.* **18**, 3015–3025 (2012).
16. Tsounis, G. & Edmunds, P. J. Three decades of coral reef community dynamics in St. John, USVI: a contrast of scleractinians and octocorals. *Ecosphere* **8**, e01646 (2017).
17. Tkachenko, K. S., Wu, B. J., Fang, L. S. & Fan, T. Y. Dynamics of a coral reef community after mass mortality of branching Acropora corals and an outbreak of anemones. *Mar. Biol.* **151**, 185–194 (2007).
18. Inoue, S., Kayanne, H., Yamamoto, S. & Kurihara, H. Spatial community shift from hard to soft corals in acidified water. *Nat. Clim. Change* **3**, 683–687 (2013).
19. Zapata, F. et al. Phylogenomic analyses support traditional relationships within Cnidaria. *PLoS ONE* **10**, e0139068 (2015).
20. Kayal, E. et al. Phylogenomics provides a robust topology of the major cnidarian lineages and insights on the origins of key organismal traits. *BMC Evol. Biol.* **18**, 68 (2018).
21. Xiao, M. et al. Mitogenomics suggests a sister relationship of *Relicanthus daphneae* (Cnidaria: Anthozoa: Hexacorallia: *incerti ordinis*) with Actiniaria. *Sci. Rep.* **9**, 18182 (2019).
22. McFadden, C. S., France, S. C., Sánchez, J. A. & Alderslade, P. A. Molecular phylogenetic analysis of the Octocorallia (Cnidaria: Anthozoa) based on mitochondrial protein-coding sequences. *Mol. Phylogenet. Evol.* **41**, 513–527 (2006).
23. Berntson, E. A., Bayer, F. M., McArthur, A. G. & France, S. C. Phylogenetic relationships within the Octocorallia (Cnidaria: Anthozoa) based on nuclear 18S rRNA sequences. *Mar. Biol.* **138**, 235–246 (2001).
24. Medina, M., Collins, A. G., Takaoka, T. L., Kuehl, J. V. & Boore, J. L. Naked corals: skeleton loss in Scleractinia. *Proc. Natl Acad. Sci. USA* **103**, 9096–9100 (2006).
25. Bayer, F. M. & Macintyre, I. G. The mineral component of the axis and holdfast of some gorgonacean octocorals (Coelenteratea: Anthozoa), with special reference to the family Gorgoniidae. *Proc. Biol. Soc.* **103**, 205–228 (2001).
26. Gabay, Y., Fine, M., Barkay, Z. & Benayahu, Y. Octocoral tissue provides protection from declining oceanic pH. *PLoS ONE* **9**, e91553 (2014).
27. Purgstaller, B., Mavromatis, V., Immenhauser, A. & Dietzel, M. Transformation of Mg-bearing amorphous calcium carbonate to Mg-calcite—in situ monitoring. *Geochim. Cosmochim. Acta* **174**, 180–195 (2016).
28. Ries, J. B. Effect of ambient Mg/Ca ratio on Mg fractination in calcareous marine invertebrates: a record of the oceanic Mg/Ca ratio over the Phanerozoic. *Geology* **32**, 981–984 (2004).
29. Conci, N., Wörheide, G. & Vargas, S. New non-bilaterian transcriptomes provide novel insights into the evolution of coral skeletomes. *Genome Biol. Evol.* **11**, 3068–3081 (2019).
30. Drake, J. L. et al. How corals made rocks through the ages. *Glob. Change Biol.* **26**, 31 (2019).
31. Tambutté, S. et al. Coral biomineralization: from the gene to the environment. *J. Exp. Mar. Biol. Ecol.* **408**, 58–78 (2011).
32. Sevilgen, D. S. et al. Full in vivo characterization of carbonate chemistry at the site of calcification in corals. *Sci. Adv.* **5**, eaau7447 (2019).
33. Higuchi, T., Shirai, K., Mezaki, T. & Yuyama, I. Temperature dependence of aragonite and calcite skeleton formation by a scleractinian coral in low mMg/Ca seawater. *Geology* **45**, 1087–1090 (2017).
34. Higuchi, T. et al. Biotic control of skeletal growth by scleractinian corals in aragonite–calcite seas. *PLoS ONE* **9**, e91021 (2014).
35. Prada, C. et al. Empty niches after extinctions increase population sizes of modern corals. *Curr. Biol.* **26**, 3190–3194 (2016).
36. Stanley, G. D., Shepherd, H. M. E. & Robinson, A. J. Paleoecological response of corals to the end-triassic mass extinction: an integrational analysis. *J. Int. Earth Sci.* **29**, 879–885 (2018).
37. Kiessling, W. & Aberhan, M. Environmental determinants of marine benthic biodiversity dynamics through Triassic–Jurassic time. *Paleobiology* **33**, 414–434 (2007).
38. Richards, Z. T. et al. Integrated evidence reveals a new species in the ancient blue coral genus *Heliopora* (Octocorallia). *Sci. Rep.* **8**, 15875 (2018).
39. Bhattacharya, D. et al. Comparative genomics explains the evolutionary success of reef-forming corals. *eLife* **5**, e13288 (2016).
40. Squires, D. F. The evolution of the deep-sea coral family Micrabaciidae. *Stud. Trop. Oceanogr.* **5**, 502–510 (1967).
41. Guinotte, J. M. et al. Will human-induced changes in seawater chemistry alter the distribution of deep-sea scleractinian corals? *Front. Ecol. Envir.* **4**, 141–146 (2006).
42. Edmunds, P. J. & Lasker, H. R. Cryptic regime shift in benthic community structure on shallow reefs in St. John, US Virgin Islands. *Mar. Ecol. Prog. Ser.* **559**, 1–12 (2016).
43. Quattrini, A. M. et al. Universal target-enrichment baits for anthozoan (Cnidaria) phylogenomics: new approaches to long-standing problems. *Mol. Ecol. Resour.* **18**, 281–295 (2018).
44. Cowman, P. F. et al. An enhanced target-enrichment bait set for Hexacorallia provides phylogenomic resolution of the staghorn corals (Acroporidae) and close relatives. Preprint at *bioRxiv* https://www.biorxiv.org/content/10.1101/2020.02.25.965517v1 (2020).
45. Faircloth, B. C. PHYLUCE is a software package for the analysis of conserved genomic loci. *Bioinformatics* **32**, 786–788 (2016).

46. Bankevich, A. et al. SPAdes: a new genome assembly algorithm and its applications to single-cell sequencing. *J. Comput. Biol.* **19**, 455–477 (2012).

47. Stamatakis, A. RAxML version 8: a tool for phylogenetic analysis and post-analysis of large phylogenies. *Bioinformatics* **30**, 1312–1313 (2014).

48. Lanfear, R., Calcott, B., Ho, S. Y. W. & Guindon, S. PartitionFinder: combined selection of partitioning schemes and substitution models for phylogenetic analyses. *Mol. Biol. Evol.* **29**, 1695–1701 (2012).

49. Aberer, A. J., Kobert, K. & Stamatakis, A. ExaBayes: massively parallel Bayesian tree inference for the whole-genome era. *Mol. Biol. Evol.* **31**, 2553–2556 (2014).

50. Zhang, C., Rabiee, M., Sayyari, E. & Mirarab, S. ASTRAL-III: polynomial time species tree reconstruction from partially resolved gene trees. *BMC Bioinform.* **19**, 153 (2018).

51. Mai, U. & Mirarab, S. TreeShrink: fast and accurate detection of outlier long branches in collections of phylogenetic trees. *BMC Genom.* **19**, 272 (2018).

52. Junier, T. & Zdobnov, E. M. The Newick utilities: high-throughput phylogenetic tree processing in the UNIX shell. *Bioinformatics* **26**, 1669–1670 (2010).

53. Bouckaert, R. et al. BEAST2 2.5: an advanced software platform for Bayesian evolutionary analysis. *PLoS Comput. Biol.* **15**, e1006650 (2019).

54. Ho, S. Y. & Phillips, M. J. Accounting for calibration uncertainty in phylogenetic estimation of evolutionary divergence times. *Syst. Biol.* **58**, 367–380 (2009).

55. Stolarski, J. et al. The ancient evolutionary origins of Scleractinia revealed by azooxanthellate corals. *BMC Evol. Biol.* **11**, 316 (2011).

56. Oliveros, C. H. et al. Earth history and the passerine superradiation. *Proc. Natl Acad. Sci. USA* **116**, 7916–7925 (2019).

57. Sanderson, M. J. Estimating absolute rates of molecular evolution and divergence times: a penalized likelihood approach. *Mol. Biol. Evol.* **19**, 101–109 (2002).

58. Smith, S. A., Brown, J. W. & Walker, J. F. So many genes, so little time: a practical approach to divergence-time estimation in the genomic era. *PLoS ONE* **13**, e0197433 (2018).

59. Rambaut, A., Drummond, A. J., Xie, D., Baele, G. & Suchard, M. A. Posterior summarization in Bayesian phylogenetics using Tracer 1.7. *Syst. Biol.* **67**, 901 (2018).

60. Brown, J. W. & Smith, S. A. The past sure is tense: on interpreting phylogenetic divergence time estimates. *Syst. Biol.* **67**, 340–353 (2018).

61. Huelsenbeck, J. P., Nielsen, R. & Bollback, J. P. Stochastic mapping of morphological characters. *Syst. Biol.* **52**, 131–158 (2003).

62. Revell, L. J. phytools: an R package for phylogenetic comparative biology (and other things). *Methods Ecol. Evol.* **3**, 217–223 (2012).

63. Höhna, S. et al. RevBayes: Bayesian phylogenetic inference using graphical models and an interactive model-specification language. *Syst. Biol.* **65**, 726–736 (2016).

64. Harmon, L. J., Weir, J. T., Brock, C. D., Glor, R. E. & Challenger, W. GEIGER: investigating evolutionary radiations. *Bioinformatics* **24**, 129–131 (2008).

65. Höhna S. et al. Bayesian approach for estimating branch-specific speciation and extinction rates. Preprint at *bioRxiv* https://doi.org/10.1101/555805 (2019).

Author contributions

C.S.M., E.R. and A.M.Q. conceived and designed this study. A.M.Q., C.S.M., E.R., M.R.B., M.E.H. and D.A.P.-G. conducted molecular lab work. A.M.Q. conducted bioinformatic and phylogenetic analyses with guidance from B.C.F. D.A.P.-G. and P.F.C. helped with figure preparation. A.M.Q., E.R. and C.S.M. wrote the manuscript. M.E.H. contributed improvements to the text. P.F.C. contributed text to the supplementary file. A.M.Q., E.R., B.C.F., P.F.C., M.R.B., G.A.F., M.V.K., M.E.H., C.L.M., D.A.P.-G., J.D.R. and C.S.M. aided in interpretation of results. All authors contributed to a draft of the manuscript and approved the final version of the manuscript.

Competing interests

The authors declare no competing interests

Additional information

Extended data is available for this paper at https://doi.org/10.1038/s41559-020-01291-1.

Supplementary information is available for this paper at https://doi.org/10.1038/s41559-020-01291-1.
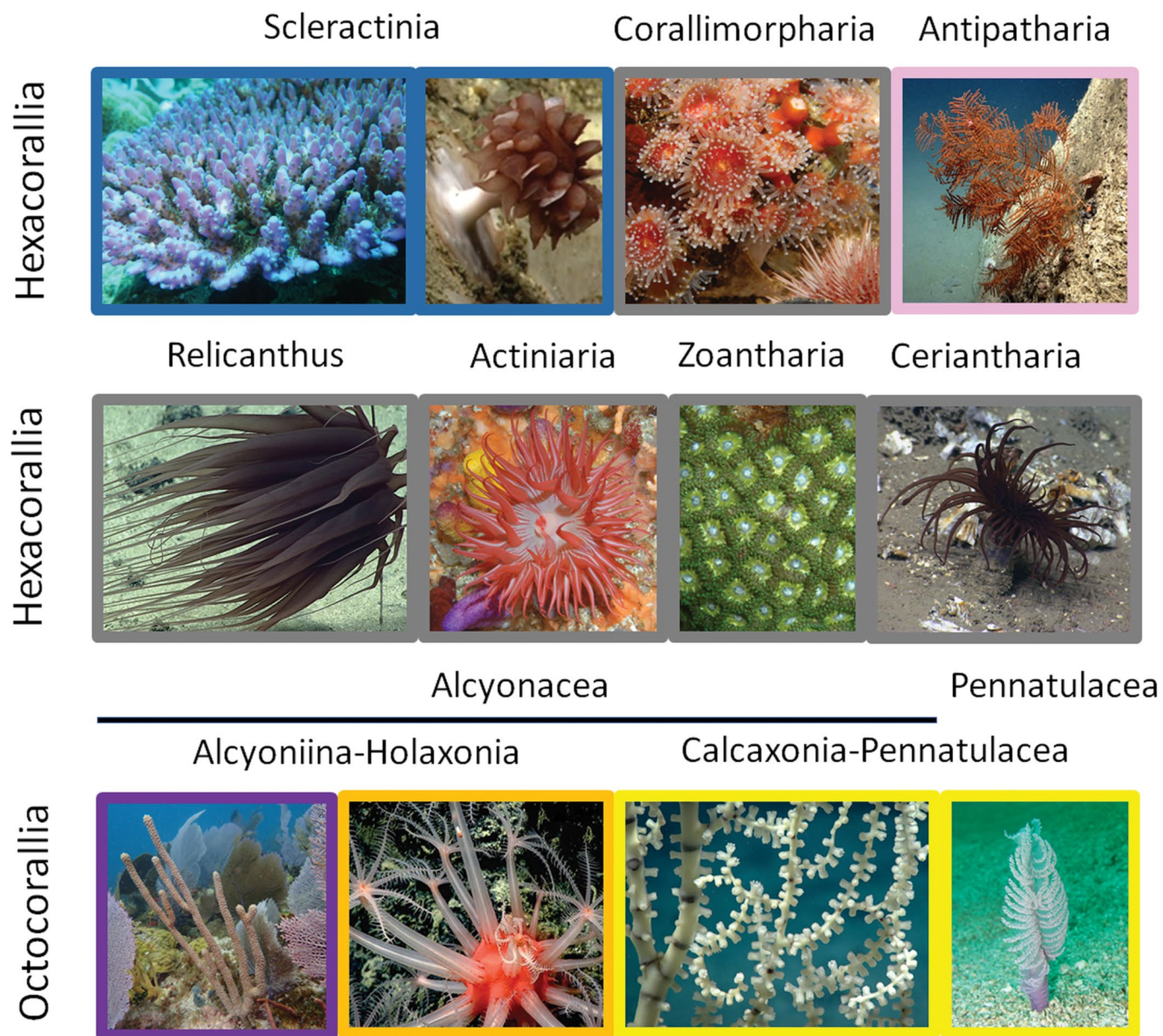
Correspondence and requests for materials should be addressed to A.M.Q.

**Peer review information** Peer reviewer reports are available.

Reprints and permissions information is available at www.nature.com/reprints.

Publisher's note Springer Nature remains neutral with regard to jurisdictional claims in published maps and institutional affiliations.

Extended Data Fig. 1 | Photographs of anthozoans. *Acropora* sp. (Scleractinia, stony coral), *Javania* sp. (Scleractinia, solitary stony coral), *Corynactis annulata* (Corallimorpharia, naked coral), *Telopathes magna* (Antipatharia, black coral); Hexacorals middle row, left to right: *Relicanthus* cf. *daphneae* (Actiniaria, anemone), Actiniidae sp. (Actiniaria, anemone), *Zoanthus sansibaricus* (Zoantharia, colonial anemone), Ceriantharia (Ceriantharia, tube anemone); Octocorals bottom row, left to right: *Plexaurella nutans* and *Gorgonia ventalina* (Alcyonacea, holaxonian gorgonians), *Anthomastus* sp. (Alcyonacea, soft coral), Keratoisidinae (Alcyonacea, calcaxonian gorgonian), *Virgularia* cf. *gustaviana* (Pennatulacea, sea pen). Photographs taken by C.S. McFadden, J. D. Reimer, or courtesy of NOAA Office of Ocean Exploration and Research.
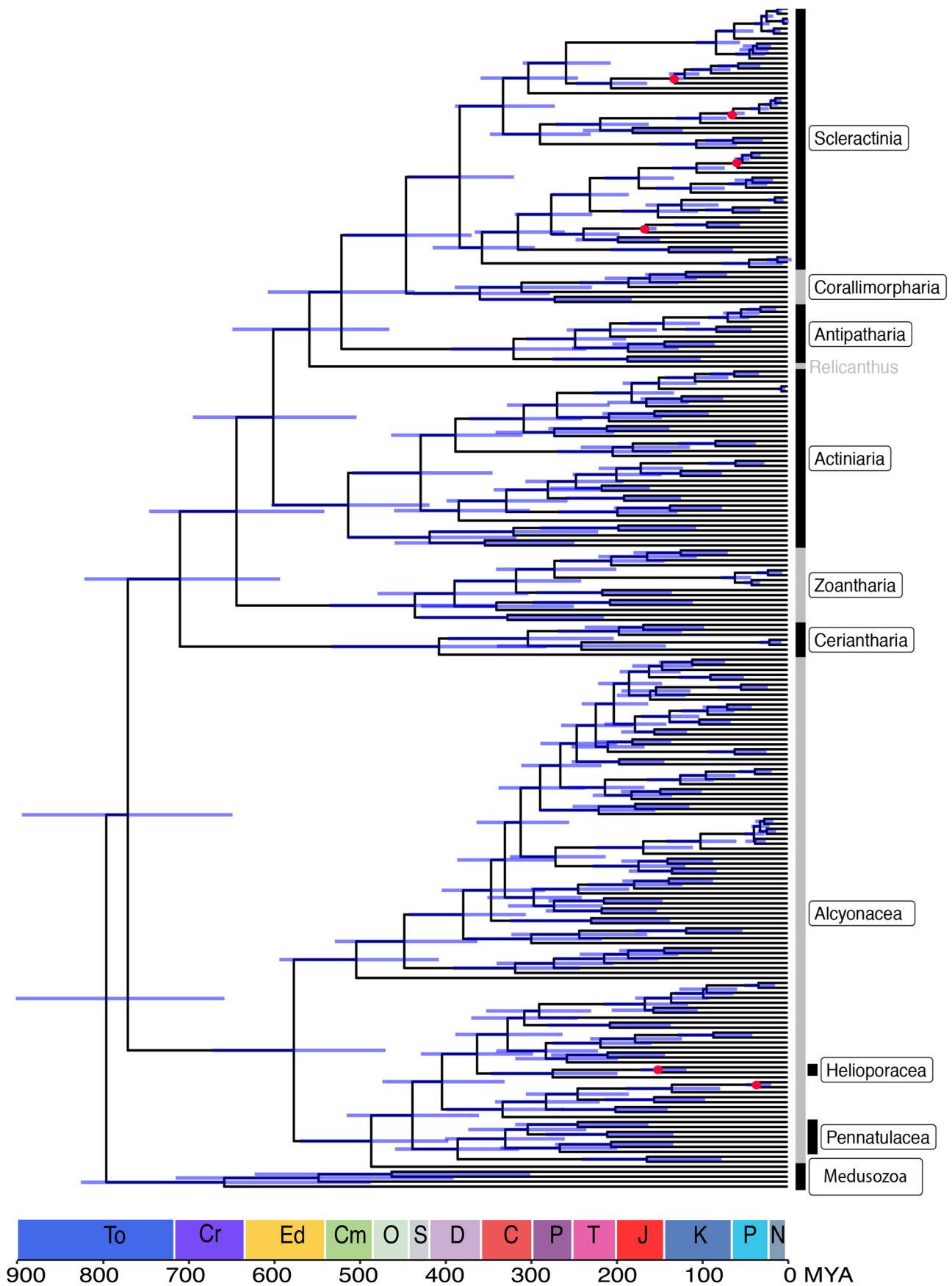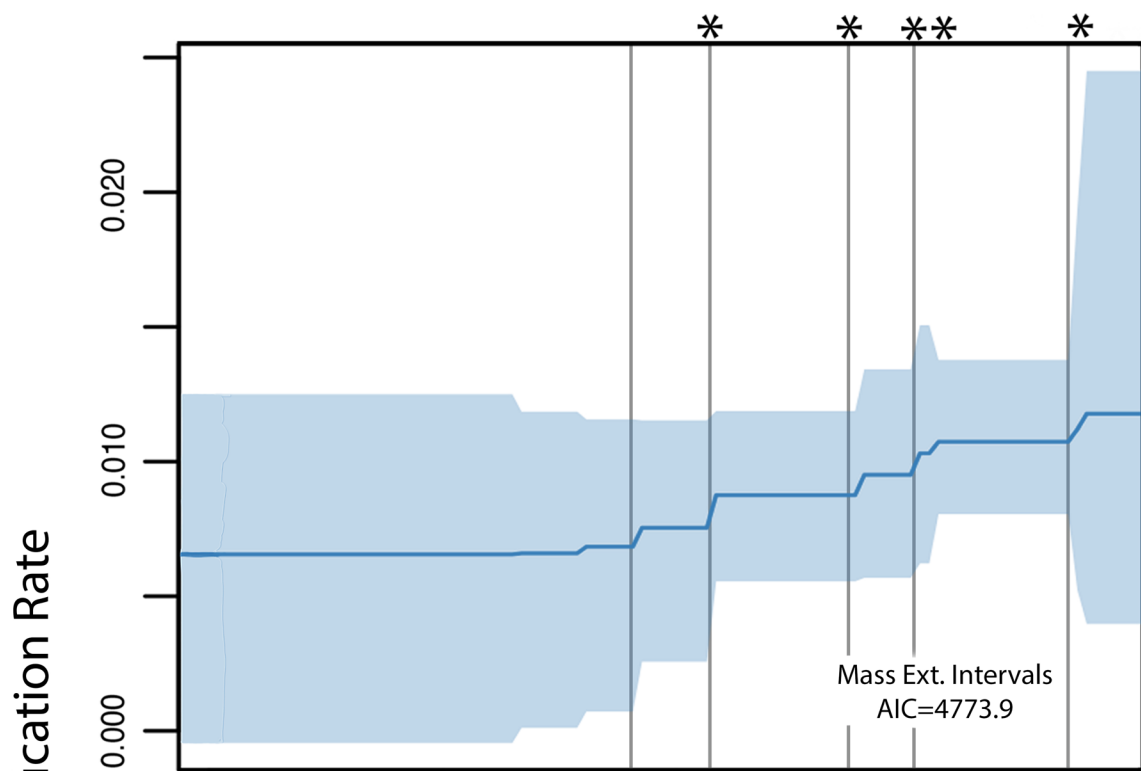
Extended Data Fig. 2 | Time-calibrated phylogeny. BEAST2 dated phylogeny with 95% highest posterior densities (blue bars) of node ages and red circles to denote fossil calibration points.
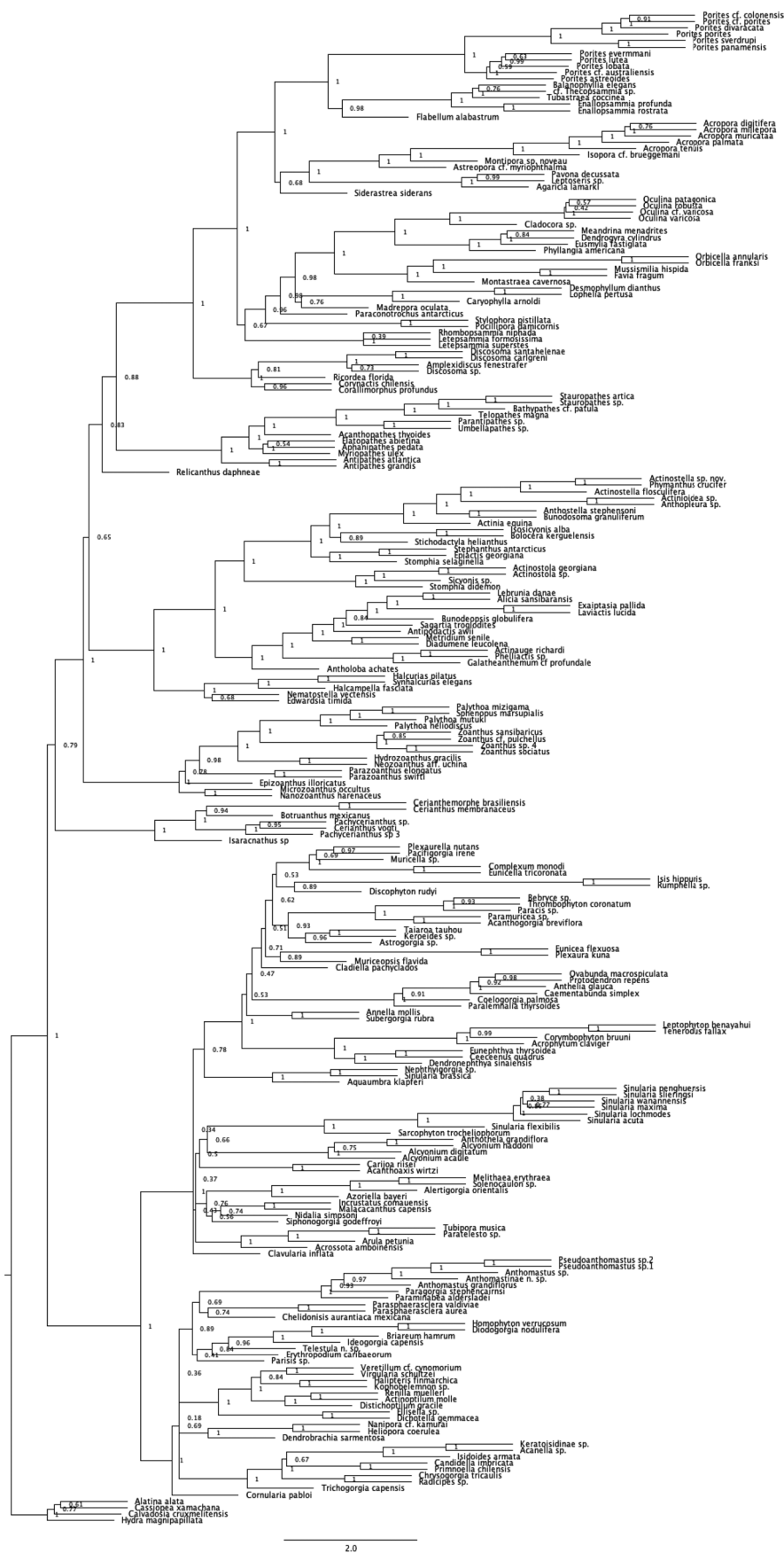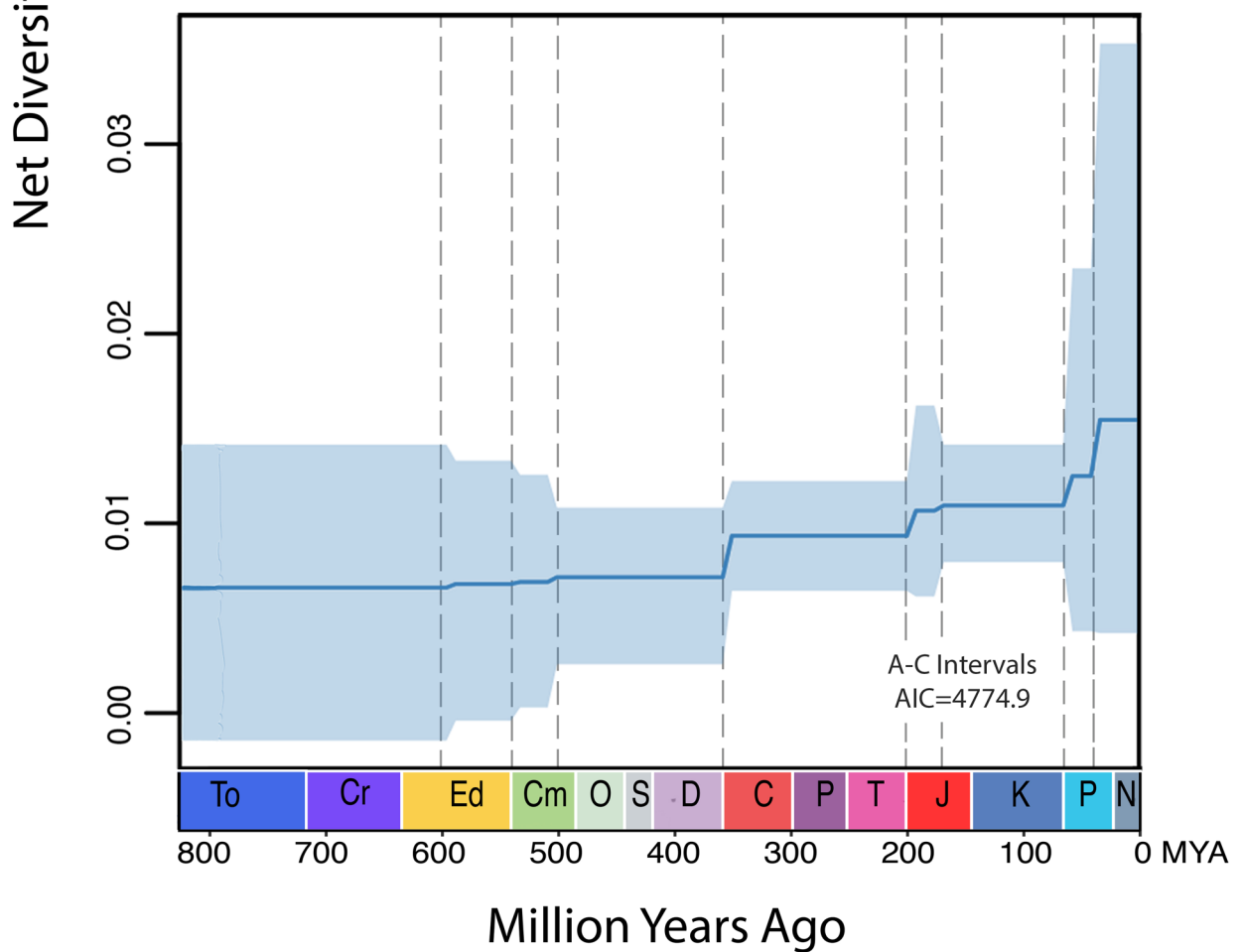
**Extended Data Fig. 3 | Species tree.** ASTRAL III species tree with posterior probabilities calculated in ASTRAL.

Extended Data Fig. 4 | Net diversification rates. Net diversification rates (speciation minus extinction) across deep time. A) calculated between mass extinction events (solid lines) and reef crises (*), and B) between aragonite-calcite sea intervals (dotted lines).
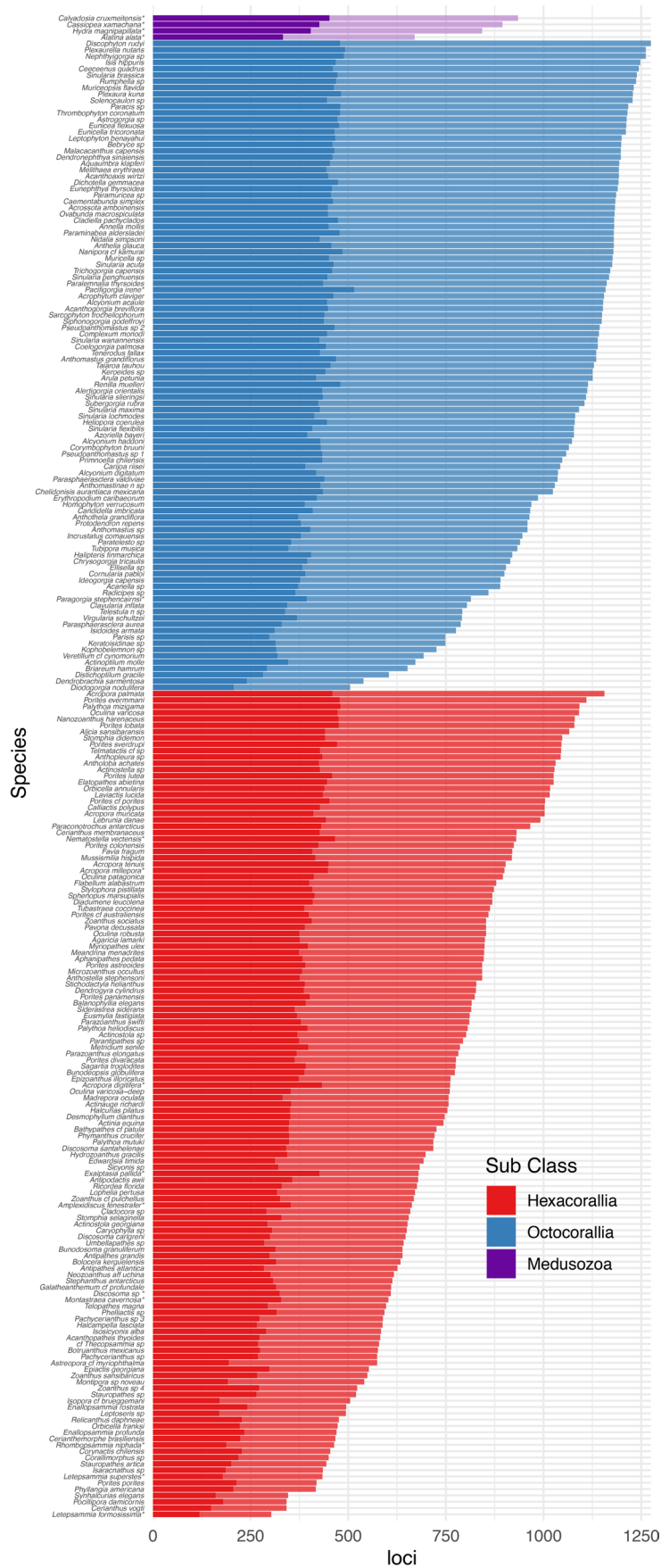
Extended Data Fig. 5 | Locus recovery per species. Number of loci recovered for each species in anthozoan sub-classes and class Medusozoa. *=loci extracted from genomes.

nature research

Corresponding author(s):   Andrea Quattrini

Last updated by author(s):   03-30-2020

Reporting Summary

Nature Research wishes to improve the reproducibility of the work that we publish. This form provides structure for consistency and transparency in reporting. For further information on Nature Research policies, see Authors & Referees and the Editorial Policy Checklist.

Statistics

For all statistical analyses, confirm that the following items are present in the figure legend, table legend, main text, or Methods section.

n/a	Confirmed	
☒	☐	The exact sample size (n) for each experimental group/condition, given as a discrete number and unit of measurement
☒	☐	A statement on whether measurements were taken from distinct samples or whether the same sample was measured repeatedly
☒	☐	The statistical test(s) used AND whether they are one- or two-sided *Only common tests should be described solely by name; describe more complex techniques in the Methods section.*
☒	☐	A description of all covariates tested
☒	☐	A description of any assumptions or corrections, such as tests of normality and adjustment for multiple comparisons
☒	☐	A full description of the statistical parameters including central tendency (e.g. means) or other basic estimates (e.g. regression coefficient) AND variation (e.g. standard deviation) or associated estimates of uncertainty (e.g. confidence intervals)
☒	☐	For null hypothesis testing, the test statistic (e.g. F, t, r) with confidence intervals, effect sizes, degrees of freedom and P value noted *Give P values as exact values whenever suitable.*
☐	☒	For Bayesian analysis, information on the choice of priors and Markov chain Monte Carlo settings
☒	☐	For hierarchical and complex designs, identification of the appropriate level for tests and full reporting of outcomes
☒	☐	Estimates of effect sizes (e.g. Cohen's d, Pearson's r), indicating how they were calculated

Our web collection on statistics for biologists contains articles on many of the points above.

Software and code

Policy information about availability of computer code

Data collection	We used code in the phyluce package, which is available freely on line to obtain loci from our samples.
Data analysis	We used freely available software programs and/or code to analyze data. All programs and R packages are provided in the text with relevant citations or with links to access the code. Additional code can be found in the code file on figshare.

For manuscripts utilizing custom algorithms or software that are central to the research but not yet described in published literature, software must be made available to editors/reviewers. We strongly encourage code deposition in a community repository (e.g. GitHub). See the Nature Research guidelines for submitting code & software for further information.

Data

Policy information about availability of data

All manuscripts must include a data availability statement. This statement should provide the following information, where applicable:
- Accession codes, unique identifiers, or web links for publicly available datasets
- A list of figures that have associated raw data
- A description of any restrictions on data availability

Raw Data: SRA Genbank SUB3122367, BioSample #SAMN07774920-4952, 13244867-5050
Anthozoan bait set: Data Dryad Entry http://dx.doi.org/10.5061/dryad.36n40
Alignment and tree files, BEAST2 xml and result files: figshare https://doi.org/10.6084/m9.figshare.12363953

Field-specific reporting

Please select the one below that is the best fit for your research. If you are not sure, read the appropriate sections before making your selection.

☐ Life sciences   ☐ Behavioural & social sciences   ☒ Ecological, evolutionary & environmental sciences

For a reference copy of the document with all sections, see nature.com/documents/nr-reporting-summary-flat.pdf

Ecological, evolutionary & environmental sciences study design

All studies must disclose on these points even when the disclosure is negative.

Study description	A phylogenomic study of corals and their relatives (class Anthozoa, phylum Cnidaria) across deep time
Research sample	This work is focused on the class Anthozoa (corals, sea anemones) in the phylum Cnidaria. We used 234 specimens collected across the world over the past ~30 years. Locations and dates of collections are included in Supplementary Table 1.
Sampling strategy	Our strategy was to use specimens from all orders and most families of anthozoans to ensure complete representation across the phylogeny.
Data collection	We used specimens collected worldwide over the past ~30 years in our phylogenetic analyses.
Timing and spatial scale	not applicable
Data exclusions	Because a few clades were sampled more frequently at the species-level than other clades, we pruned tips in the phylogeny to one species per genus for the branch-specific rate diversification analyses.
Reproducibility	not applicable
Randomization	not applicable
Blinding	not applicable

Did the study involve field work?   ☐ Yes   ☒ No

Reporting for specific materials, systems and methods

We require information from authors about some types of materials, experimental systems and methods used in many studies. Here, indicate whether each material, system or method listed is relevant to your study. If you are not sure if a list item applies to your research, read the appropriate section before selecting a response.

Materials & experimental systems

n/a	Involved in the study
☒	☐ Antibodies
☒	☐ Eukaryotic cell lines
☒	☐ Palaeontology
☐	☒ Animals and other organisms
☒	☐ Human research participants
☒	☐ Clinical data

Methods

n/a	Involved in the study
☒	☐ ChIP-seq
☒	☐ Flow cytometry
☒	☐ MRI-based neuroimaging

Animals and other organisms

Policy information about studies involving animals; ARRIVE guidelines recommended for reporting animal research

Laboratory animals	not applicable
Wild animals	not applicable
Field-collected samples	This study involved specimens collected over the past ~30 years from a variety of sources (including museum material). No field work was conducted for this present study. Often, only small clippings of the animal were collected and preserved in the field.
Ethics oversight	not applicable-invertebrates

Note that full information on the approval of the study protocol must also be provided in the manuscript.